

Hard Ferromagnetic Behavior in Atomically Thin CrSiTe₃ Flakes

Cheng Zhang^{+1,4}, Le Wang^{+2,3}, Yue Gu⁵, Xi Zhang⁶, Xiuquan Xia^{2,3}, Shaolong Jiang⁴, Liang-Long Huang^{2,3}, Ying Fu^{2,3}, Cai Liu^{2,3}, Junhao Lin⁴, Xiaolong Zou⁵, Huimin Su^{*2,3}, Jia-Wei Mei^{*2,4,3,7}, Jun-Feng Dai^{*2,3,8}

1. School of Physics, Harbin Institute of Technology, Harbin, 150001, China
2. Shenzhen Institute for Quantum Science and Engineering, Southern University of Science and Technology, Shenzhen, 518055, China
3. International Quantum Academy, Shenzhen, 518048, China
4. Department of Physics, Southern University of Science and Technology, Shenzhen, 518055, China
5. Shenzhen Geim Graphene Center, Tsinghua-Berkeley Shenzhen Institute & Tsinghua Shenzhen International Graduate School, Tsinghua University, Shenzhen 518055, China
6. Shannxi Institute of Flexible Electronics, Northwestern Polytechnical University, Xi'an 710072, China
7. Shenzhen Key Laboratory of Advanced Quantum Functional Materials and Devices, Southern University of Science and Technology, Shenzhen 518055, China
8. Shenzhen Key Laboratory of Quantum Science and Engineering, Shenzhen 518055, China

Supporting Information

1. Synthesis of CrSiTe₃ single crystals

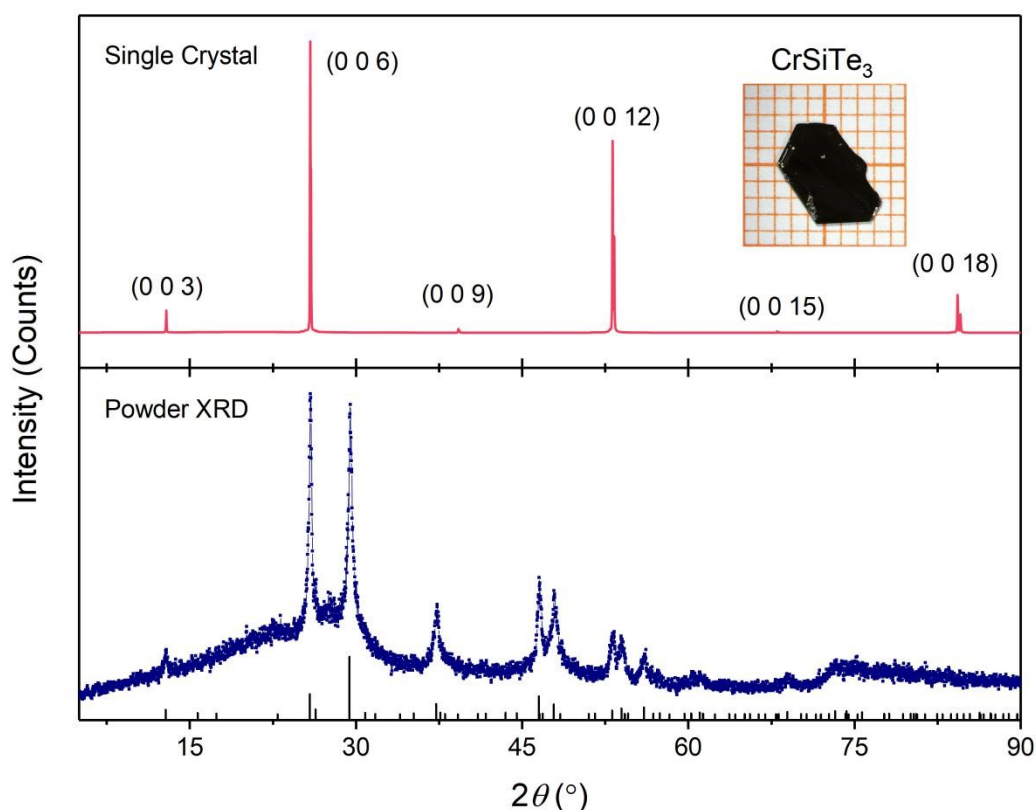


Figure S1 The single crystal and powder X-ray diffraction pattern of CrSiTe₃. The black bars in the lower panel are the simulated X-ray diffraction peaks.

CrSiTe₃ crystals were grown using the Si-Te eutectic as flux. High-purity elements Cr grains (99.996%), Si pieces (99.9999%), Te blocks (99.9999%) were weighed in the molar ratio Cr:Si:Te = 1:2:6, and placed in an alumina crucible, then sealed in a fully evacuated quartz tube. The crucible was heated to 1373 K and dwell for 10 hrs, then cooled slowly to 973 K within 150 hrs, where the flux was spun off by a centrifuge. Large hexagonal black single crystals can be obtained, as shown in the inset of Figure S1. The single crystal XRD and powder

(obtained by grinding the single crystals) XRD were performed on a Rigaku Smartlab-9kW diffractometer with Cu $K\alpha$ radiation ($\lambda_{K\alpha 1} = 1.54056 \text{ \AA}$) at room temperature. The powder XRD, obtained by grinding the single crystals, is consistent with the simulated one (R-3, No. 148, $a = 6.7578 \text{ \AA}$, and $c = 20.6650 \text{ \AA}$), suggesting that our samples adopt the same structure. The flat hexagonal surfaces were identified as the (0 0 3) planes.

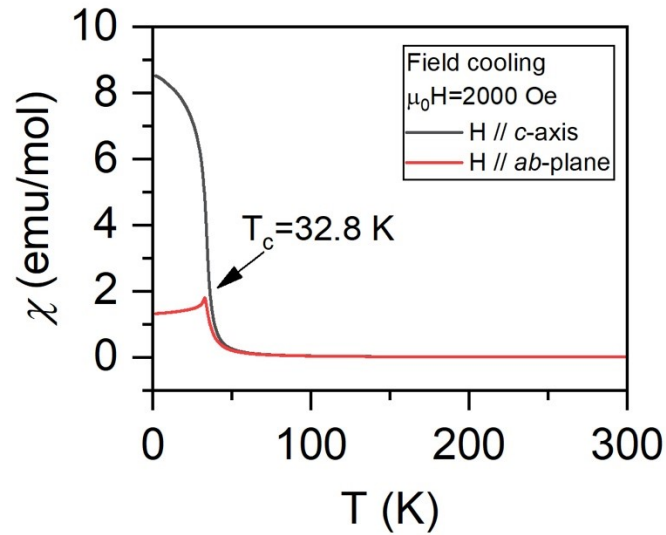
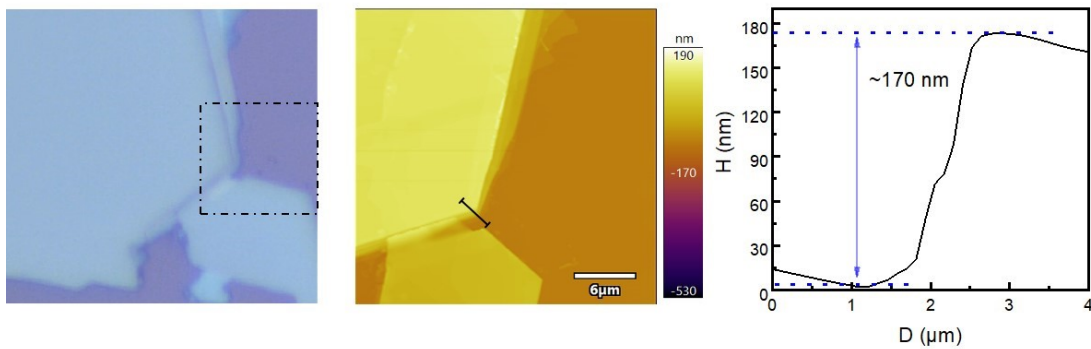
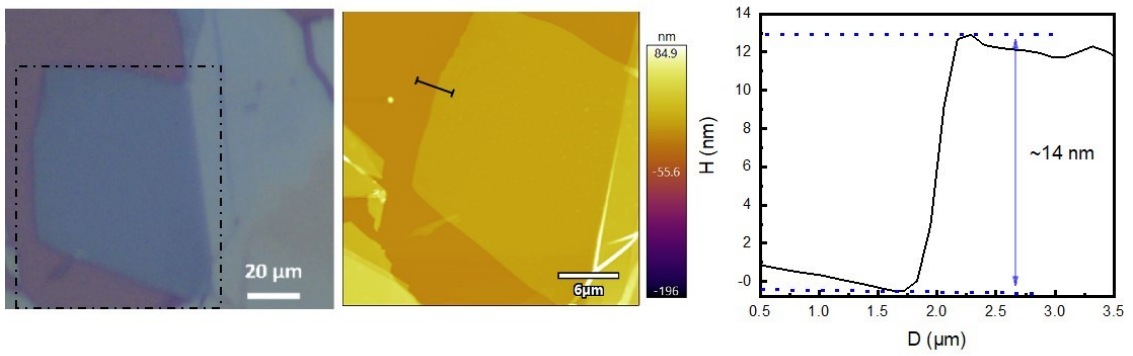
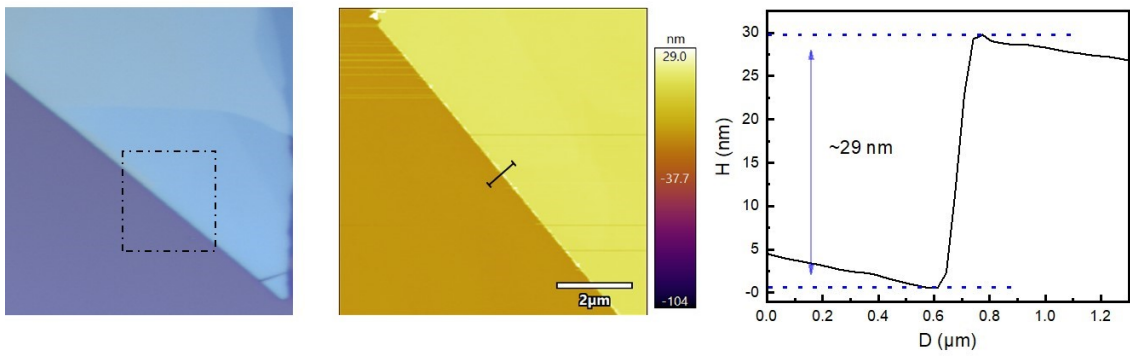
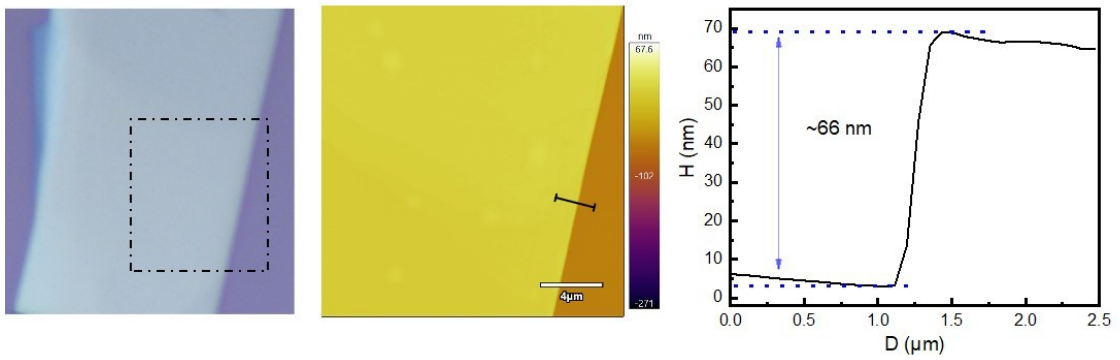
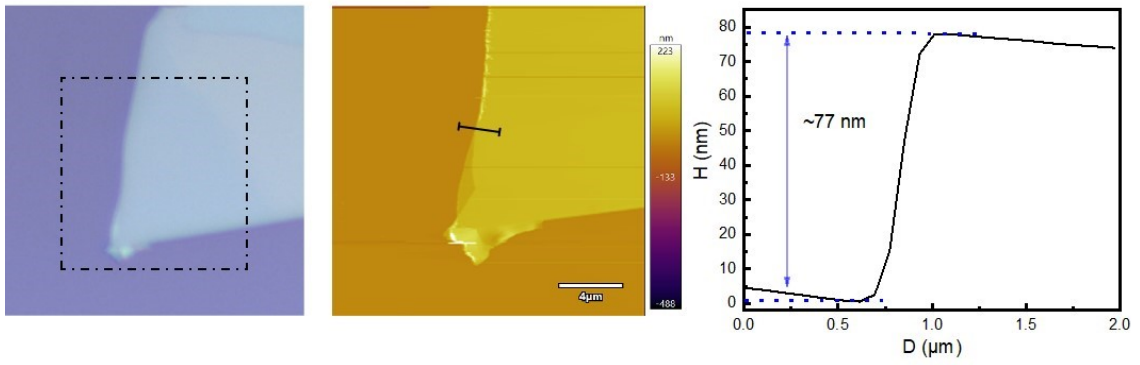
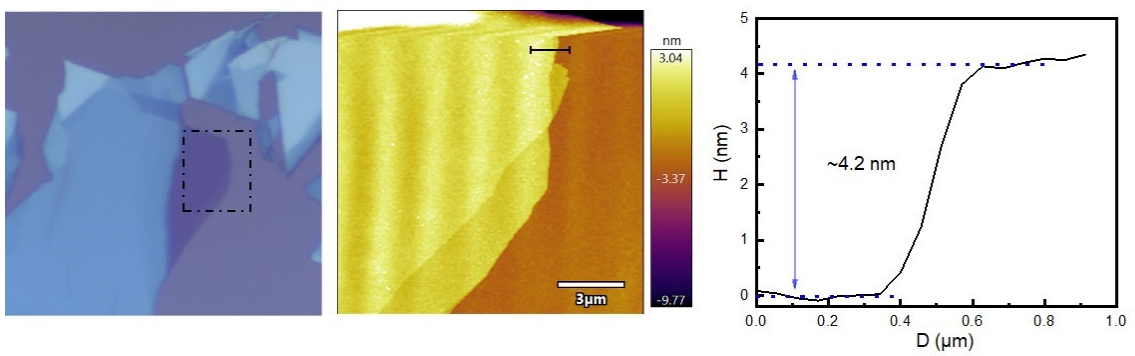
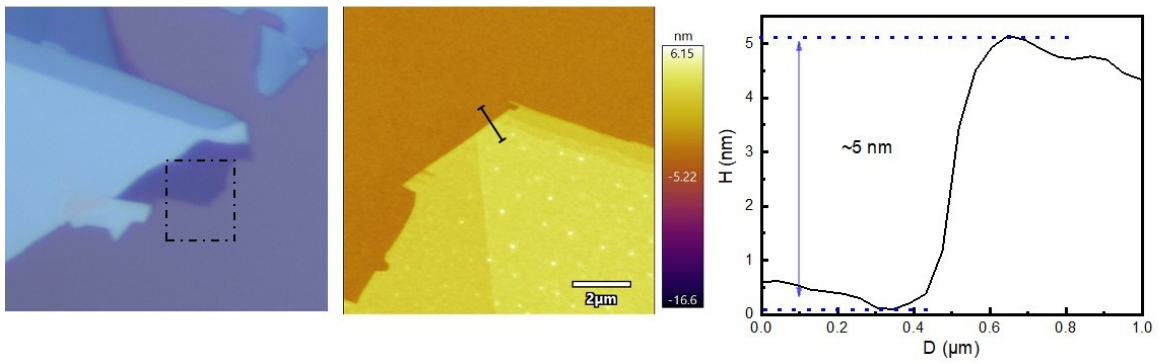
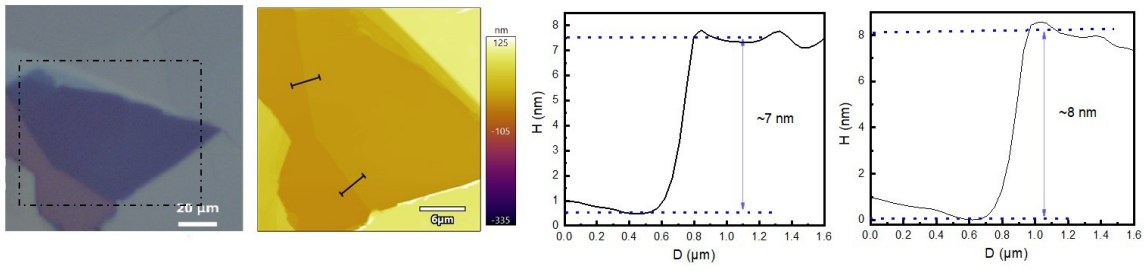
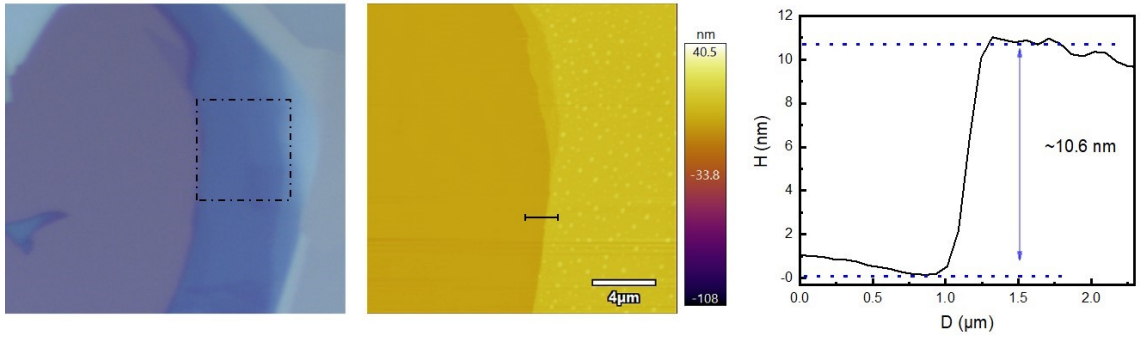


Figure S2 Magnetic susceptibility of CrSiTe₃ measured on a single crystal at the field cooling (FC) along the c-axis (black curve) and ab-plane (red curve), respectively.

2. Optical image and AFM measurements







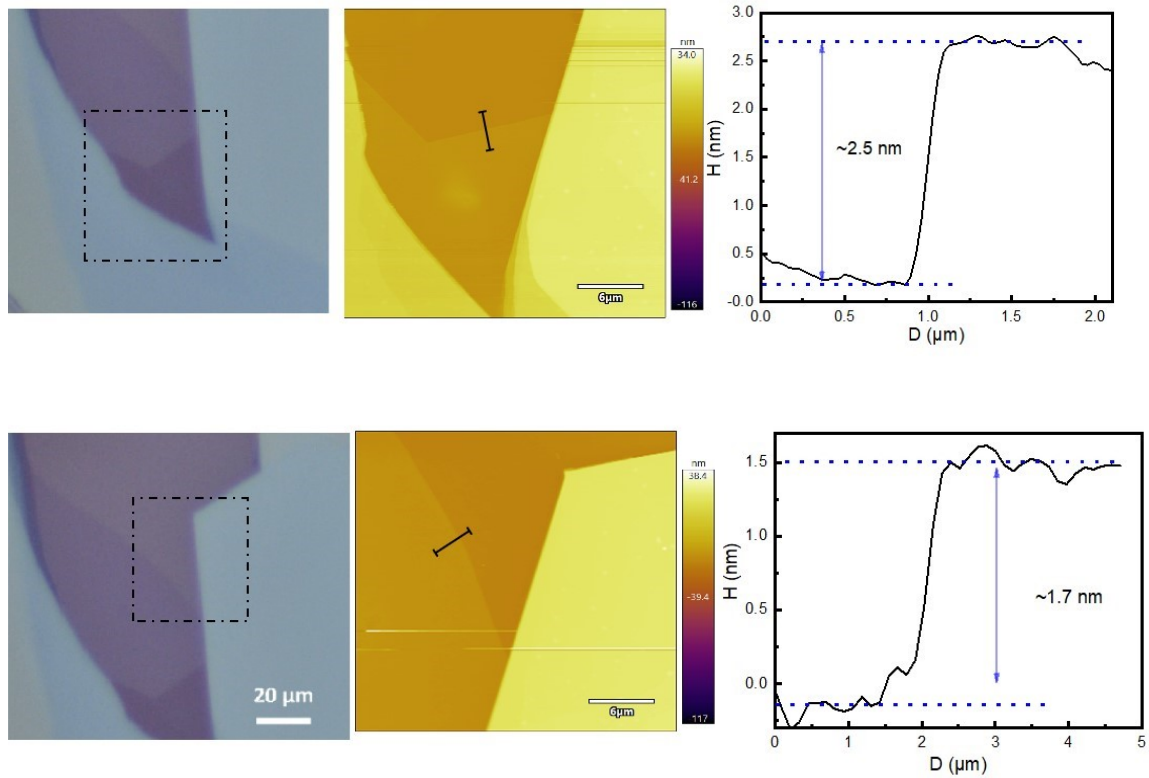


Figure S3: Optical and AFM images for CrSiTe₃ samples with different thicknesses.

3. Sample installation

We have designed a special sample holder with a lid, which can fit into the cold-finger of cryostat. Because there is an optical window in the middle of lid, we can conduct the spectral measurements. First, we stuck the sample onto the surface of holder and capped it with the lid in the glove box. Therefore, the space stored sample was also filled with nitrogen. And then we took out the holder and fixed it to the cold-finger of low-temperature cryostat. During installation, the sample was always immersed in nitrogen atmosphere. After vacuum-pumping, the nitrogen in the holder can be pumped out. Therefore, we can avoid any possible air pollution during sample transfer.

4. MCD measurements

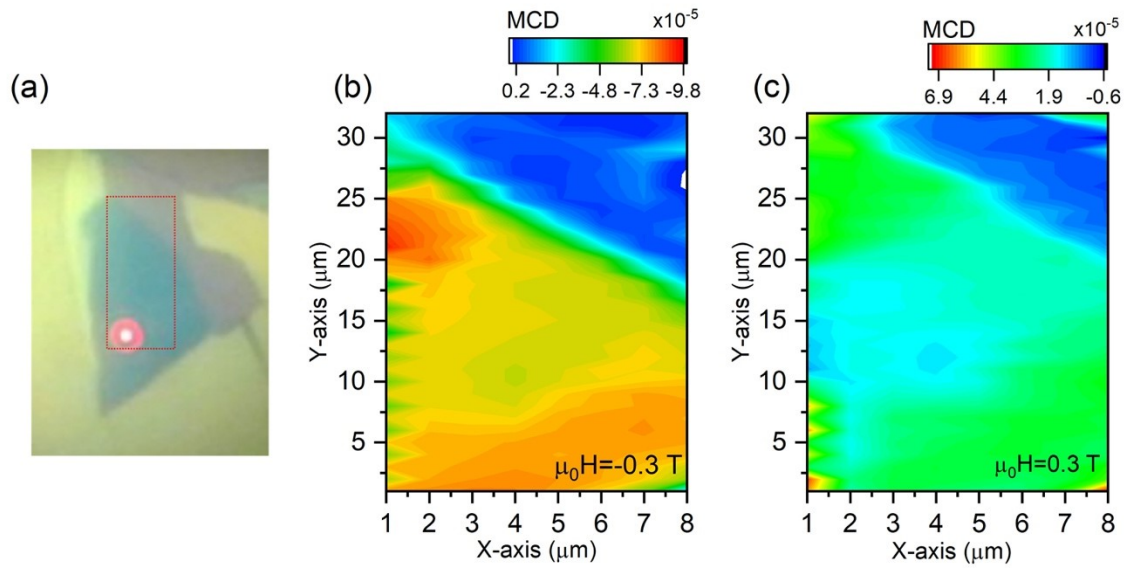


Figure S4: (a) Optical image of the 7 (and 8) nm CrSiTe₃ sample. Red dashed square indicates the mapping range. MCD mapping in the sample under (b) $\mu_0 H = -0.3 \text{ T}$ and (c) $\mu_0 H = 0.3 \text{ T}$, respectively. Since this sample contains two regions, e.g., 7 and 8 nm parts, the intensity difference of MCD signal may originate from different regions.

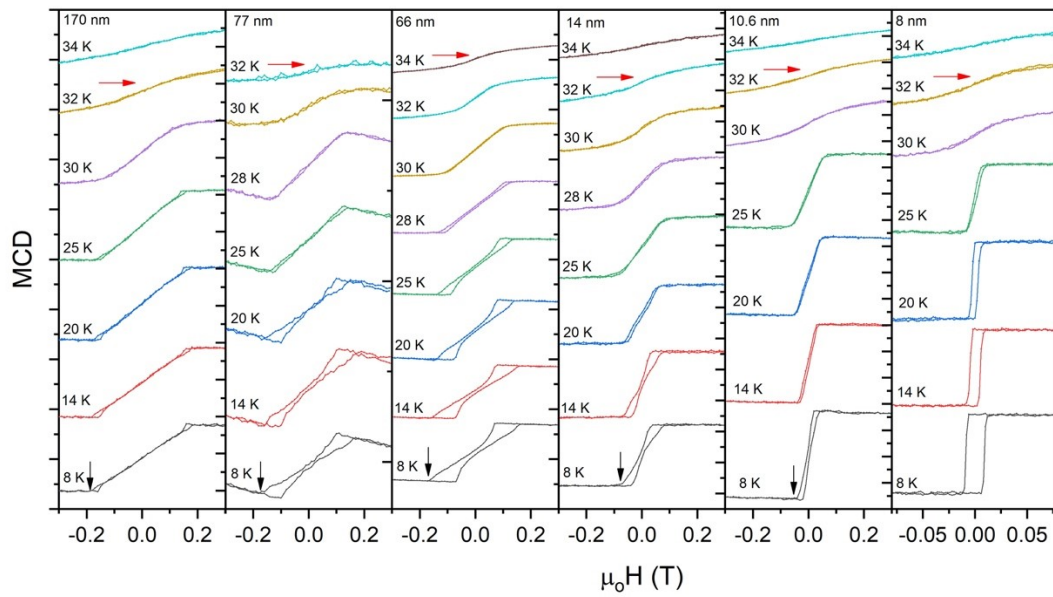


Figure S5: Temperature dependence of MCD signal in samples with different thicknesses. The red arrows indicate the transition temperature. The black arrows indicate the saturation field.

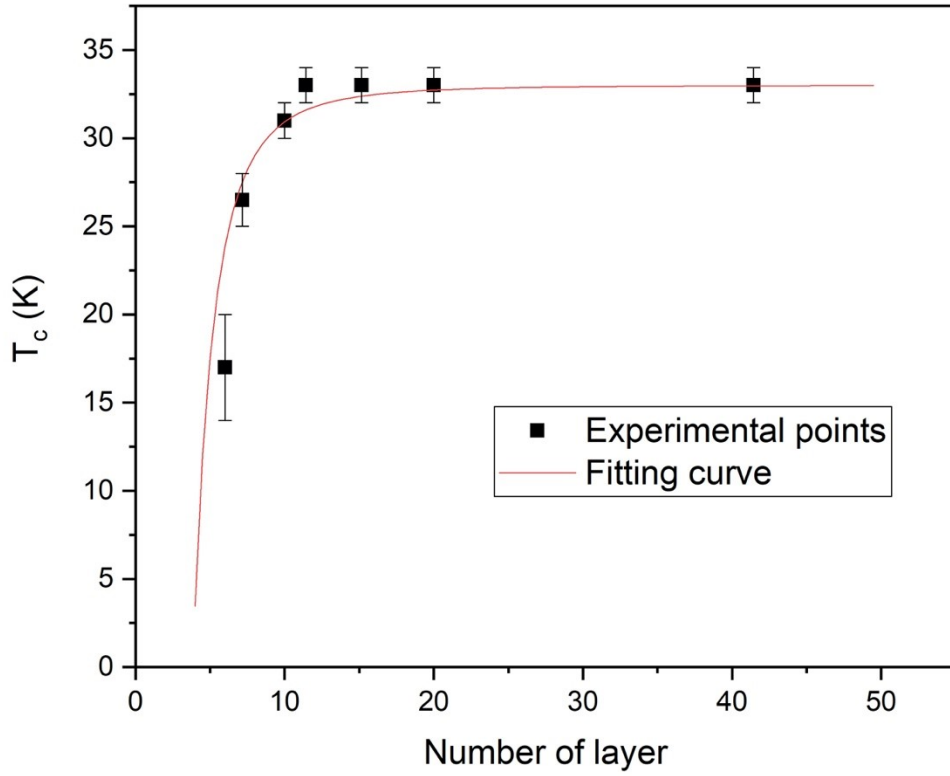


Figure S6: Extracted T_c as a function of number of layer (black squares) and the fitting curve (red line) by using $\frac{[T_c(\infty) - T_c(N)]}{T_c(\infty)} = [(N_0 + 1)/2N]^\lambda$.

5. Raman spectroscopy

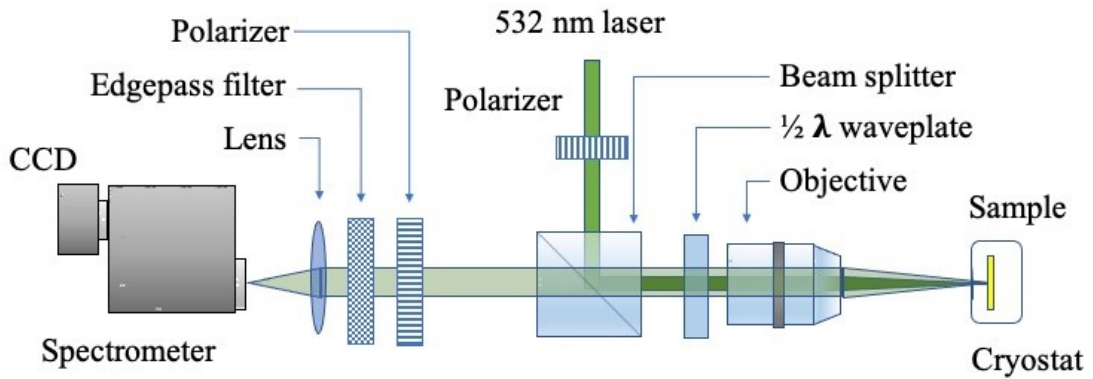


Figure S7: Schematic diagram of polarized Raman spectroscopy

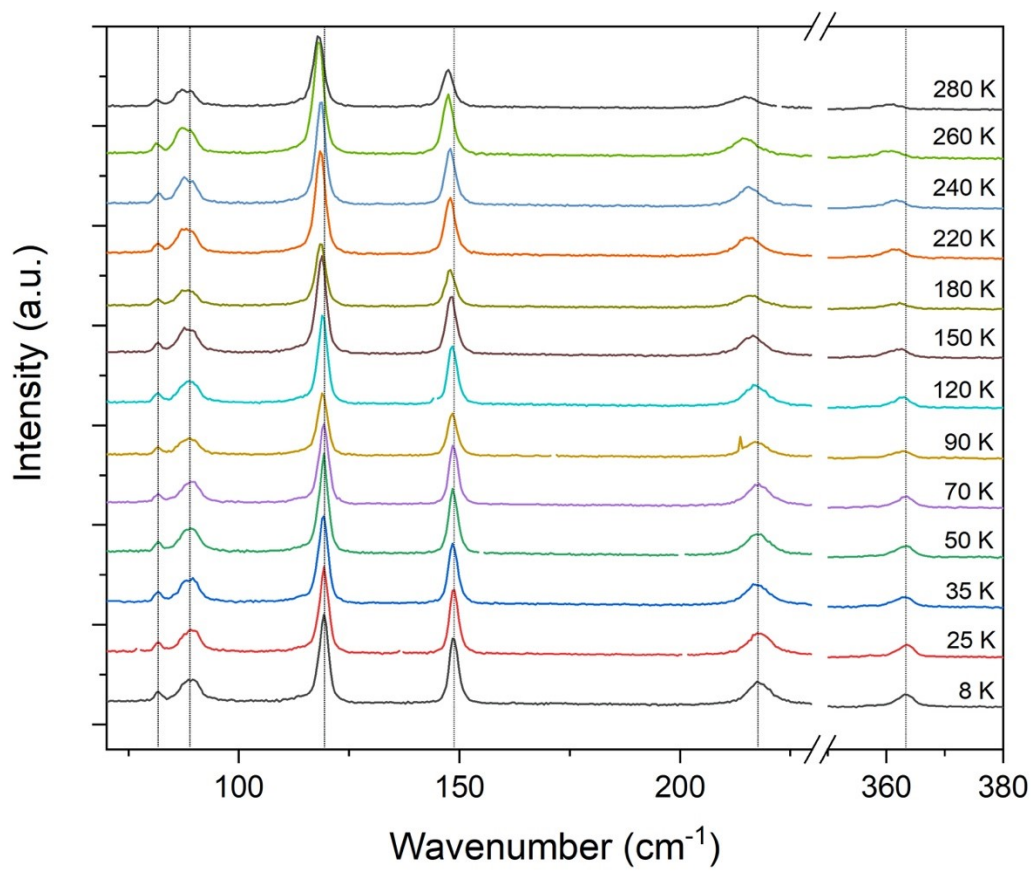


Figure S8: Temperature-dependent Raman measurement in the 14 nm CrSiTe₃.

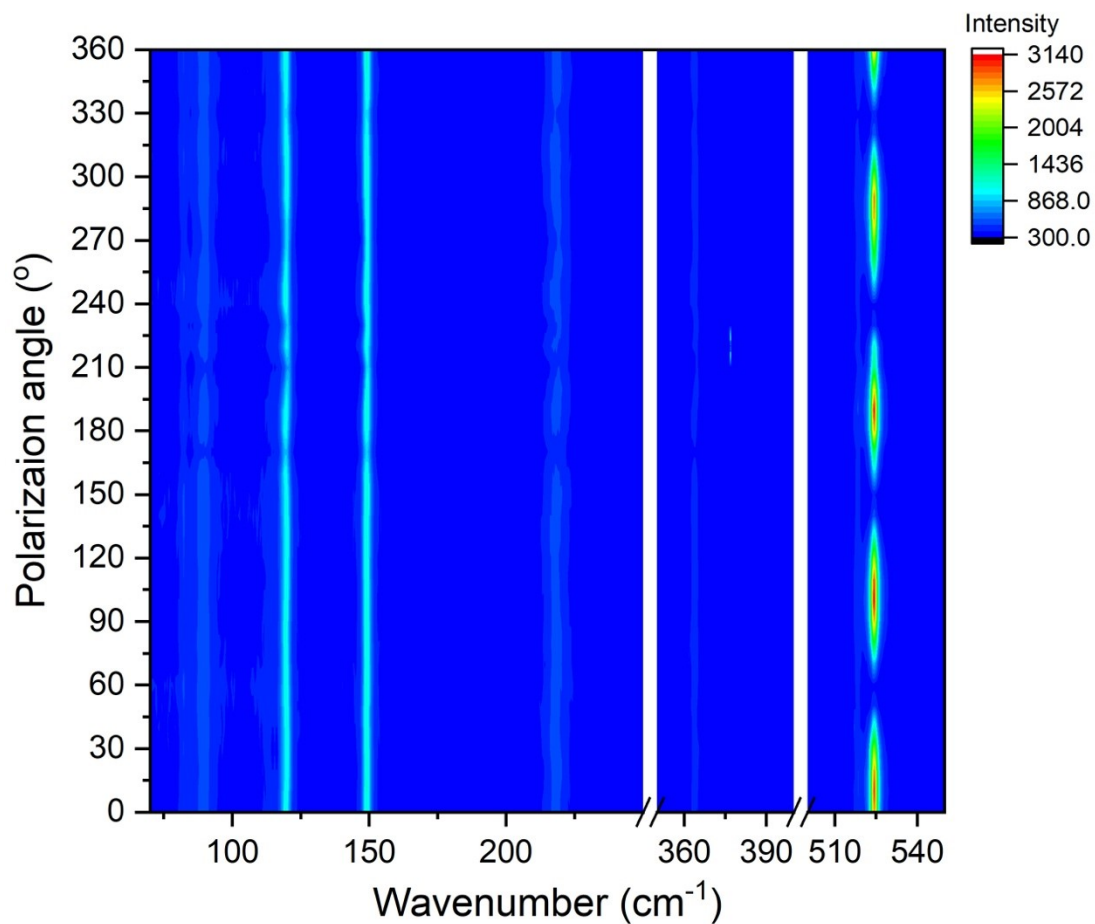


Figure S9: Polarization-dependent Raman measurement in the 14 nm CrSiTe₃ at 8 K. The peak at 525 cm⁻¹ originates from silicon substrate, which show a strong polarization-angle dependence.

6. Ferromagnetic properties for exposed CrSiTe₃

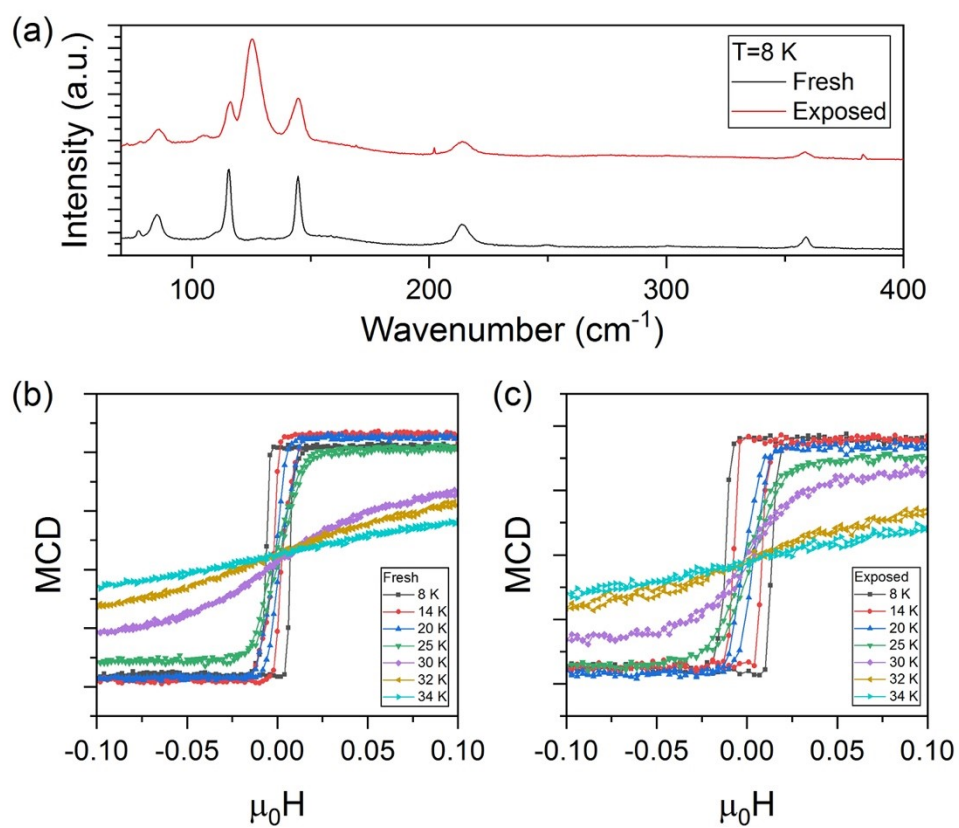


Figure S10: (a) Raman spectra of the fresh and exposed 7 nm sample. (b) and (c) are the temperature-dependent MCD measurements in the 7 nm CrSiTe_3 before and after exposure to the air.